

1-Aminoanthraquinone derivatives as a novel corrosion inhibitor for carbon steel API 5L-X60 in white petrol–water mixtures

N. Muthukumar^{a,c,*}, A. Ilangovan^b, S. Maruthamuthu^a,
N. Palaniswamy^a, A. Kimura^c

^a Central Electrochemical Research Institute, Karaikudi 630006, India

^b School of Chemistry, Bharathidasan University, Trichirappalli 620024, India

^c Institute of Advanced Energy, Kyoto University, Gokasho, Uji, Kyoto 6110011, Japan

ARTICLE INFO

Article history:

Received 25 September 2008

Received in revised form 4 December 2008

Accepted 29 December 2008

Keywords:

Organic compounds

Chemical synthesis

Atomic force microscopy (AFM)

Corrosion

ABSTRACT

Three amide derivatives of 1-aminoanthraquinones (AAQs) synthesized from long chain fatty acids were evaluated for corrosion inhibition efficiency against steel (API 5L-X60) in white petrol–water mixtures at room temperature by weight loss and electrochemical studies. Potentiodynamic polarization studies carried out at room temperature on steel (API 5L-X60) in white petrol with water containing 120 ppm of chloride and 50 ppm of the 1-aminoanthraquinone derivatives showed that all the investigated compounds are of anodic type and good corrosion inhibitors in white petrol–water mixtures. Oleic acid derivative of 1-aminoanthraquinone was found to be the best corrosion inhibitor. It exhibited 86% inhibition efficiency against the corrosion of API 5L-X60 steel. The surface analysis by AFM indicated the adsorption of inhibitors on the metal surface. Besides, all the synthesized 1-aminoanthraquinone derivatives exhibited antimicrobial efficacy against *Serratia marcescens* ACE2 and *Bacillus cereus* ACE4.

© 2009 Elsevier B.V. All rights reserved.

1. Introduction

Oil fields are the biggest victim of corrosion and severe economic loss is caused due to the metallic corrosion on piping and plant systems. Statistical data show that failures by corrosion in the oil and gas industry oscillate between 25% and 30% of the total losses [1–3]. Different methods are used for protection of corrosion in petroleum product pipeline and plants in aggressive environments, where one of the most economic methods is the application of corrosion inhibitors (CIs) [4–7]. Organic compounds used as typical oil field corrosion inhibitors function by forming a film or protective barrier between metals and the corrosive fluids either because of their anodic, cathodic or mixed type behaviour [8,9]. Alkenyl phenols [10], aromatic aldehydes [11], nitrogen containing heterocyclic and their quaternary salts [12] and condensation products of carbonyls and amines [13] are some of the commonly used oil field corrosion inhibitors. In oil transporting pipelines stagnation of water occurs due to the slopes in the landscape and it acts as breeding ground for bacteria. Now it is well established that bacterial species exist in oil pipeline and degrade petroleum to maintain their life cycle [14,15] and leads to severe corrosion problems [16].

Mitigation of oil pipeline corrosion still remains as a daunting challenge and continuous efforts are being made to solve or minimize this problem.

Quinones take part in several biological processes such as photosynthesis and respiration. In certain biomembrane assemblies they are part of electron transfer chains, for example in mitochondrial respiration, this role is played by ubiquinone or coenzyme Q [17]. Anthraquinone derivatives have been employed as dyes [18], chemical sensors [19], organogelators [20], mesogens [21–26] and anti-cancer agents [27]. We envisaged that a suitable quinone derivative, due to the inherent ability to take part in electron transfer reaction, can influence corrosion behaviour of a metal which is an electron transfer electrochemical phenomenon [28]. In this direction, on the development of novel corrosion inhibitors, three long chain fatty acid (octanoic acid, decanoic acid and oleic acid) derivatives of 1-aminoanthraquinone was synthesized (compounds 5–7) and corrosion inhibition properties on API 5L-X60 mild steel in white petrol–water mixture was evaluated. Selection of these compounds as corrosion inhibitors is based on the facts that these compounds contain lone pair of electrons on N atoms and π electrons in aromatic ring through which it can adsorb on the metal surface. The lateral interaction of long chain of carbon atoms due to Van der Waals forces can further facilitate formation of compact film of inhibitor on the metal surface [29]. In the present study, mechanism of action of 1-aminoanthraquinone derivatives as corrosion inhibitor was also investigated in white petrol–water mixtures.

* Corresponding author at: Institute of Advanced Energy, Kyoto University, Gokasho, Uji, Kyoto 6110011, Japan. Tel.: +81 774 38 3478; fax: +81 774 38 3479.

E-mail address: muthu12kumar@yahoo.co.in (N. Muthukumar).

2. Experimental work

2.1. Materials and methods

Octanoic acid, decanoic acid, oleic acid, 1-aminoanthraquinone, potassium carbonate, thionyl chloride and dimethyl formamide and acetone obtained from Aldrich were used for the synthesis of 1-aminoanthraquinone derivatives. All used solvents were of HPLC grade.

2.2. Spectral characterization of inhibitors

All the products obtained were completely characterized using nuclear magnetic resonance (NMR) spectroscopy, Fourier transform infrared spectroscopy (FT-IR) and ultra visible spectrophotometer (UV) studies. The FT-IR spectroscopy was used to detect the functional groups present in the compounds. PerkinElmer, Paragon 500 model FT-IR was used for the analysis of the corrosion inhibitors. The spectrum was taken in the mid-IR region of 400–4000 cm^{-1} with 16-scan speed. The samples were mixed with spectroscopically pure KBr in the ratio of 1:100 and pellets were fixed in the sample holder and the analyses were carried out. ^1H NMR spectra were measured in a solvent of deuterated chloroform (CDCl_3), containing 0.1% (v/v) of tetramethylsilane (TMS) as an internal standard. The chemical shifts (δ) are reported in ppm and the coupling constants (J) in Hz. All experiments were performed on a Bruker 400 MHz spectrometer. UV–vis spectra were carried out on CARY 500 scan UV–Visible spectrophotometer with CHCl_3 as solvent.

2.3. Corrosion study

The corrosion inhibition efficiency of 1-aminoanthraquinone derivatives **5–7** was evaluated using weight loss method. Steel API 5L-X60 grade (C-0.29 max, S-0.05 max, P-0.04 max, Mn-1.25 max, Fe-remaining all) coupons of size 2.5 cm (l) \times 2.5 cm (b) \times 0.5 cm (t) were mechanically polished to mirror finish and then degreased using trichloroethylene [30]. To simulate the oil field pipeline environment, control system consisting of 500 ml of oil with 2% of water containing 120 ppm of chloride ion was made. Quinone derivatives **5–7** (at different concentrations) were added in experimental system. Three mild steel specimens were immersed into each system and corrosion inhibition was evaluated by ASTM standard (G 170) reported by Papavinasam et al. [31] for the period of 10 days. After inoculation period, the coupons were removed and pickled, washed with water and dried by air drier. Final average weight loss values for three coupons were taken and the corrosion rate was calculated.

2.4. Electrochemical studies

The electrochemical experiments were carried out using a conventional three-electrode cell assembly at 28 ± 1 °C. All the solutions were prepared using AR grade chemicals using triple distilled water and deaerated by purging purified nitrogen for half an hour before the start of the experiments. The working electrode was a steel (API 5L-X60) sample of 1 cm^2 area and the rest being covered with araldite epoxy. A large rectangular platinum foil was used as counter electrode and saturated calomel electrode as the reference electrode. The working electrode was polished with different grades of emery papers, washed with water and degreased with trichloroethylene. The polarization and impedance studies were carried out after 30 min of immersion using Solatron Electrochemical Analyzer (Model 1280 B). The polarization was carried out using Corware software from a cathodic potential of -0.2V to an anodic potential of $+0.2\text{V}$ with respect to the corrosion potential at a sweep rate of 0.5mV s^{-1} . The data in the Tafel region (-0.2V to $+0.2\text{V}$ versus corrosion potential) have been processed for evaluation of corrosion kinetic parameters. The linear Tafel segments of the anodic and cathodic curves were extrapolated to corrosion potential for obtaining the corrosion current values.

The inhibition efficiency was evaluated from the measured I_{corr} values using the relationship (Eq. (1)):

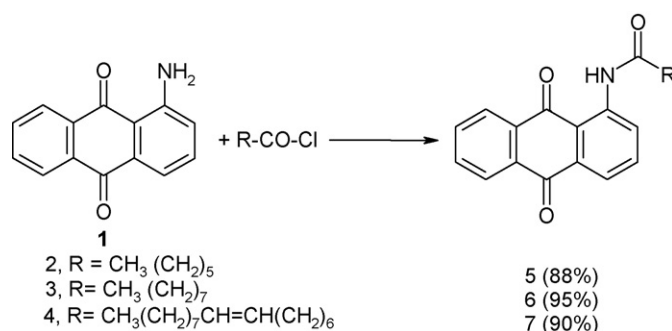
$$\text{IE\%} = \frac{I_{\text{corr}} - I_{\text{corr}}'}{I_{\text{corr}}} \times 100 \quad (1)$$

where I_{corr} and I_{corr}' are the corrosion current values without and with the addition of various concentrations of 1-aminoanthraquinone derivatives.

The impedance measurements were carried out using ac signals of 10 mV amplitude for the frequency spectrum from 100 kHz to 0.01 Hz. Marquardt's model [32] based on Taylor series expansion, a non-linear fitting technique was applied for calculating impedance parameters. A mixture of petroleum and water (containing 120 ppm chloride ion) in the ratio of 2:1 was made [33]. In each system two mild steel specimens were immersed and stirred vigorously for a period of 7 days. After the test period, electrochemical tests were carried out in a special cell containing aqueous medium collected from the experimental system. Impedance and polarization measurements were carried out by employing water obtained after 7 days period of stirring.

2.5. Atomic force microscope (AFM)

The API 5L-X60 specimens of size 1.0 cm \times 1.0 cm \times 0.06 cm were abraded with emery paper (grade 320–500–800) to give a homogeneous surface, then washed with



Scheme 1. Schematic diagram of synthesis of 1-aminoanthraquinone derivatives (**5–7**).

distilled water and acetone. The specimens were immersed in white petrol–water mixture prepared with and without addition of 50 mg l^{-1} 1-aminoanthraquinone (AAQ) derivatives at 30 °C for 8 h, cleaned with distilled water, dried with cold air blaster. All the specimens were characterized by atomic force microscope, pico scan 2100 model (Molecular Imaging, USA), using gold-coated SiN_3 cantilevers (force constant 3 NW^{-1}) of 30 nm tip area. AFM pictures were realized in contact mode.

2.6. Antimicrobial assessment

The strains *Serratia marcescens* ACE2 and *Bacillus cereus* ACE4 were used in this study were isolated from oil transporting pipeline of oil refineries in Northwest India. (The nucleotide sequences data have been deposited in GenBank under the sequence numbers DQ092416 and AY912105). The antimicrobial properties of the synthesized 1-aminoanthraquinone derivatives were evaluated using a 100 ppm concentration [34]. The antimicrobial assay consists of 5 ml of white petrol, 5 ml of minimal media (Bushnell-Haas broth) and AAQ derivatives containing 10^7 colony-forming units (CFU) ml^{-1} of *S. marcescens* ACE2 (Gram-negative) and *B. cereus* ACE4 (Gram-positive) were inoculated separately. In control system, the growth of bacteria was checked without the addition of AAQ derivatives. After 24 h, 1 ml white petrol was serially diluted by sterilized distilled water to 9 ml by pour plate technique [34]. 1 ml of the dilution were placed onto a nutrient agar plate and incubated at 37 °C for 24 h for bacterial enumeration.

2.7. X-ray diffraction (XRD) study

A computer controlled X-ray diffraction technique, JEOL Model JDX-8030 was used to scan the corrosion products between 10° and 80° 2θ with copper $\text{K}\alpha$ radiation (Ni filter) at a rating of 40 kV, 20 mA. The dried corrosion products were collected, crushed into a fine powder and used for XRD analysis for determining the nature of film present on the metal surface.

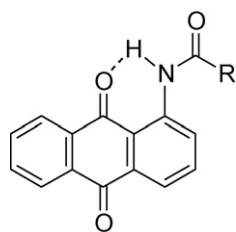
3. Results and discussion

3.1. Synthesis of inhibitors

Literature methods already known for the synthesis of 1-stearoyl, 1-palmitoyl and 1-lauroyl derivatives of 1-aminoanthraquinone or its closely related variants reveal that the products were obtained only in poor yield, ranging from 2% to 6.5%. Moreover solvent such as nitromethane was used which is difficult to purify at the workup stage [35]. Similarly 1,4-diaminoanthraquinone derivatives were prepared, only in moderate yield, by treatment of 1,4-diaminoanthraquinone with acyl chlorides in the presence of pyridine and N,N-dimethylacetamide as solvent [36]. Based on this background we have planned for an improved procedure for the synthesis of 1-aminoanthraquinone derivatives **5–7**. Accordingly, 1-aminoanthraquinone was treated with acid chlorides **2–4** in the presence of potassium carbonate (K_2CO_3), in acetone at reflux temperature to give corresponding amides in very good yield (Scheme 1). Acid chlorides were prepared by treatment of corresponding acid with equivalent quantity of thionyl chloride (SOCl_2). All the products were obtained as yellow solid with characteristic melting point.

3.2. Characterization of inhibitors

All the 1-aminoanthraquinone derivatives were characterized using NMR, FT-IR and UV studies. Introduction of long alkyl chain



Scheme 2. Intramolecular hydrogen bonding of 1-aminoanthraquinone derivatives (5–7).

gave raise to good solubility for 1-aminoanthraquinone derivatives 5–7 in non-polar organic solvents, such as benzene, toluene and tetrahydrofuran (THF). The solubility increased proportionately with increase in alkyl chain length. As such 1-aminoanthraquinone is not freely soluble in organic solvents such as chloroform, ethylacetate and hexane.

The ^1H NMR spectrum of AAQ derivatives 5–7, recorded in CDCl_3 , shows a triplet in the region of 0.919–0.858 ppm which is characteristic of terminal $-\text{CH}_3$ group. The multiplet in the region of 1.32–1.38 ppm and 1.78–1.85 ppm corresponds to the presence of several $-\text{CH}_2$ groups. The $-\text{CH}_2$ protons adjacent to carbonyl group appears as a triplet at 2.59 ppm. The anthraquinone aromatic ring protons appear as a multiplet in the range of 9.13–9.15 ppm, 8.92–8.26 ppm, 8.08–8.03 ppm and 7.85–7.72 ppm. The amide proton appears as a singlet at 12.35 ppm. Thus we confirmed the integration of long alkyl chain to the 1-aminoanthraquinone core unit.

IR spectra for compounds 5–7, showed $-\text{N}-\text{H}$ signals in the range at $3208\text{--}3350\text{ cm}^{-1}$ indicating primary amine was transformed into amide. The wave numbers corresponding to amide $-\text{C}=\text{O}$, hydrogen bonded quinone $\text{C}=\text{O}$ and non-hydrogen bonded quinone $\text{C}=\text{O}$ could be observed in the region $1701\text{--}1703\text{ cm}^{-1}$, $1665\text{--}1668\text{ cm}^{-1}$ and $1643\text{--}1645\text{ cm}^{-1}$ respectively. In general $-\text{C}=\text{O}$ frequency for non-hydrogen bonded secondary amides carbonyl is observed in the range $1680\text{--}1630\text{ cm}^{-1}$, in solid state. Higher wave numbers, $1701\text{--}1703\text{ cm}^{-1}$, observed for the amide $-\text{C}=\text{O}$ in compounds 5–7, show that the double bond character is further strengthened due to the influence of strong electron withdrawing nature of quinone function. In similar systems it was reported that intramolecular hydrogen bonding was reason for this kind of shift [37].

Scheme 2 shows the type of intramolecular hydrogen bonding between amide proton and one of the quinone $-\text{C}=\text{O}$ in 1-aminoanthraquinone derivatives 5–7. The introduction of strong electron withdrawing amide group lead to the hypsochromic yellow shift in absorption frequencies as noticed from its UV spectral data. This could be also due to amide $-\text{C}=\text{O}$ competing with quinone $-\text{C}=\text{O}$ group and weaken the intramolecular hydrogen bonding. Our observation supports the observations made by Philipova et al. [38]

3.2.1. Preparation of octanoic acid (9,10-dioxo-9,10-dihydroanthracen-1-yl)-amide (5)

Part 1: Preparation of octanoyl chloride—A solution of octanoic acid (3.25 g, 0.0225 mole) and four drops of DMF in benzene (10 ml)

was taken in a two necked round bottom flask equipped with a condenser, guard tube and a dropping funnel. Thionyl chloride (2.67 g, 0.0225 mole) was added slowly through dropping funnel to the reaction mixture as the reaction becomes endothermic. Stirred for 10 min and heated in an oil bath for 1 h at 60°C . The octanoyl chloride thus prepared was taken as such for further reaction which is followed in part 2.

Part 2: Preparation of octanoic acid (9,10-dioxo-9,10-dihydroanthracen-1-yl)-amide (5)—A mixture of 1-aminoanthraquinone 1 (3 g, 0.0134 mole) and K_2CO_3 (3.68 g, 0.0268 mole) in acetone (30 ml) was taken in round bottom flask equipped with guard tube and a dropping funnel and stirred at room temperature for 45 min. Octanoyl chloride in benzene, prepared as described in part 1, was added during 15 min to the reaction mixture. Reaction mixture was stirred at reflux temperature for 6 h (TLC, hexane:ethyl acetate, 7:3, $R_f=0.4$) and then allowed to attain room temperature. Poured into water (100 ml) and solid separated was extracted with ethyl acetate (4×20 ml) using a separating funnel. The combined organic layer was washed with saturated NaHCO_3 (2×20 ml) solution, dil. HCl (2×20 ml) and water (20 ml) then dried with Na_2SO_4 . Ethyl acetate was evaporated to afford octanoic acid (9,10-dioxo-9,10-dihydroanthracen-1-yl)-amide in 95% yield as a yellow solid. M.P. $132\text{--}134^\circ\text{C}$.

IR (KBr): 3235.29 cm^{-1} ($-\text{N}-\text{H}$ str), 2926.26 cm^{-1} ($-\text{C}-\text{H}$ str), 1702 cm^{-1} (amide $>\text{C}=\text{O}$), 1643.53 cm^{-1} (quinone $>\text{C}=\text{O}$), 1667.57 cm^{-1} , 1579.57 cm^{-1} , 1528.88 cm^{-1} (aromatic $-\text{C}-\text{H}$) and 1266.88 cm^{-1} ($-\text{C}-\text{N}$ bond).

UV (CHCl_3): 330 (2.50) and 414 (4.49).

^1H NMR (400 MHz, CDCl_3): δ 12.351 (s, 1H), 9.119–9.151 (m), 8.924–8.261 (m), 8.081–8.036 (m), 7.859–7.729 (m, 7H attached to C_2 , C_3 , C_4 , C_5 , C_6 , C_7 , C_8), 2.592 (t, 2H), 1.859–1.788 (m, 2H), 1.385–1.320 (m, 8H), 0.919–0.858 (t, 3H).

The same methodology was adopted for the preparation of compounds 6 and 7 (decanoic acid and oleic acid substituted aminoanthraquinone derivatives).

3.3. Corrosion study

Corrosion inhibition efficiency for quinone derivatives 5–7 was evaluated using gravimetric method. The results observed (Table 1) show that this is the first time a quinone derivative was found to show corrosion inhibition properties in white petrol pipeline environment. As the chain length increases the corrosion inhibition efficiency increased proportionately and the highest efficiency being observed for compound 7 with C_{18} side chain (84%). It gives rise to indirect indication that as compounds 5–7 binds to the metal surface large surface coverage is possible with compounds possessing long alkyl chain.

3.4. Electrochemical study

The potentiodynamic polarization behaviour in the Tafel region for steel (API 5L-X60) in white petrol–water mixture, with and without the addition of various concentrations of 1-aminoanthraquinone derivatives is shown in Figs. 1–3. The polar-

Table 1
Corrosion inhibition efficiency of AAQ derivatives (compounds 5–7) evaluated by weight loss method.

Concentration (ppm)	Octanoic acid substituted (C_8) AAQ (compound 5)		Decanoic acid substituted (C_{10}) AAQ (compound 6)		Oleic acid substituted (C_{18}) AAQ (compound 7)	
	Corrosion rate (mm year^{-1})	IE (%)	Corrosion rate (mm year^{-1})	IE (%)	Corrosion rate (mm year^{-1})	IE (%)
Blank	0.4924	–	0.4924	–	0.4924	–
25	0.3164	36	0.2544	48	0.1343	73
50	0.2739	51	0.2159	56	0.0969	81
100	0.2349	52	0.1954	60	0.0779	84

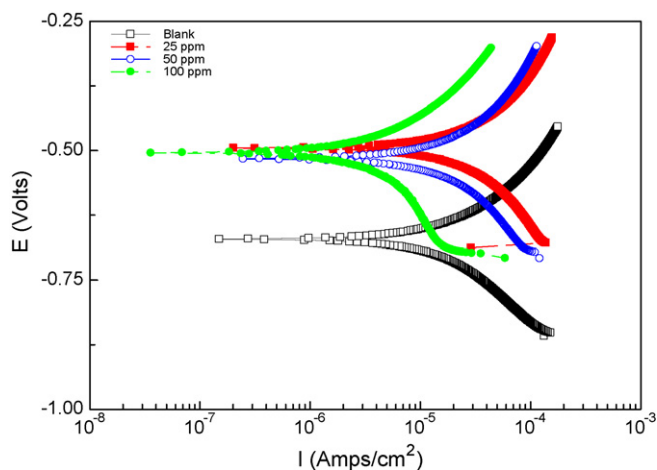


Fig. 1. Polarization behaviour of carbon steel API 5L-X in white petrol–water mixtures—effect of AAQ derivative (compound 5).

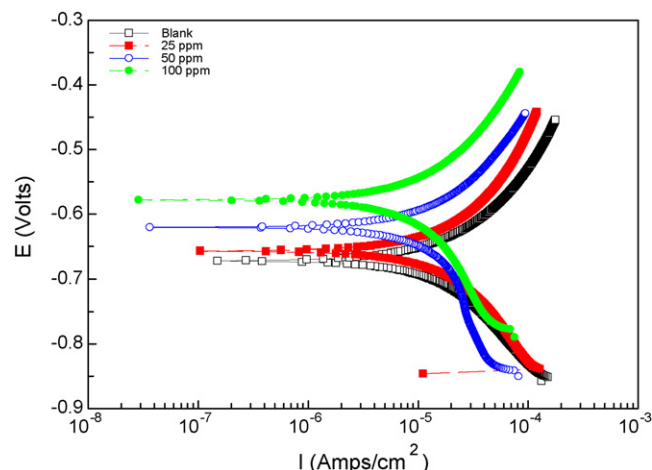


Fig. 3. Polarization behaviour of carbon steel API 5L-X in white petrol–water mixtures—effect of AAQ derivative (compound 7).

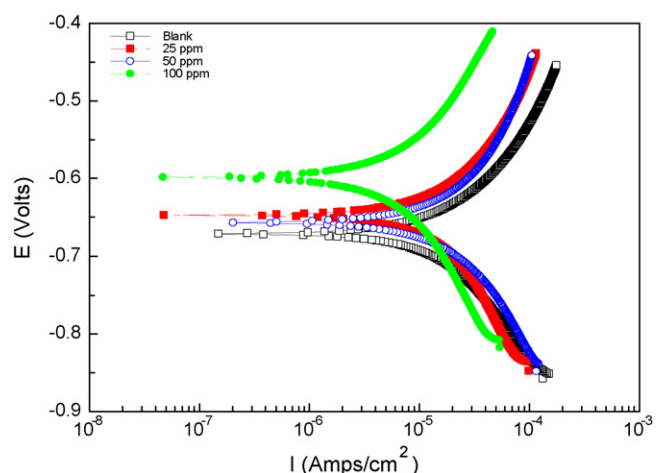


Fig. 2. Polarization behaviour of carbon steel API 5L-X in white petrol–water mixtures—effect of AAQ derivative (compound 6).

ization parameters such as corrosion potential (E_{corr}), corrosion current density (I_{corr}) and Tafel constants (b_a and b_c) were derived from these figures and are given in Table 2. In the case of 1-aminoanthraquinone derivatives 5–7, the inhibition efficiencies increased with increasing concentration. The result reveals that compound 7 has good corrosion inhibition efficiency when compared to other compounds 5 and 6. These results, together with the E_{corr} displacement towards more positive values are indicative of an effective inhibition of the carbon steel corrosion. Besides,

Table 2

Electrochemical parameters for the corrosion of carbon steel API 5L-X60 in white petrol–water mixtures—effect of AAQ derivatives (compounds 5–7).

Concentration of AAQ derivatives (ppm)	E_{corr} (mV SCE ⁻¹)	b_a (mV dec ⁻¹)	b_c (mV dec ⁻¹)	I_{corr} ($\mu\text{A cm}^{-2}$)
Blank	-671	168	176	29.2
Compound 5				
25	-515	199	215	26.1
50	-504	157	203	18.2
100	-495	199	215	4.39
Compound 6				
25	-647	185	233	19.2
50	-656	210	196	16.6
100	-598	184	210	6.46
Compound 7				
25	-656	193	197	17.9
50	-620	174	196	16.3
100	-577	172	213	10.7

they are in good agreement with those obtained from weight loss measurements.

The Nyquist plots of the impedance values of the steel (API 5L-X60) in white petrol–water mixtures with and without the addition of various concentrations of 1-aminoanthraquinone derivatives are presented in Figs. 4–6 and in Table 3. Marquardt's model [32] based on Taylor series expansion, a non-linear fitting technique was applied to find the capacitance loops in inhibitor system and control system. Single capacitive loop was noticed in the absence of inhibitor system (blank). Two capacitive loops were noticed while adding the inhibitor. The first capacitive loop in the high frequency (HF) range of the Nyquist diagram was not

Table 3

Impedance data for carbon steel API 5L-X in white petrol–water mixtures—effect of AAQ derivatives (compounds 5–7).

Compounds	Concentration (ppm)	R_{HF} ($\Omega \text{ cm}^2$)	C_{HF} (F cm^2)	R_{LF} ($\Omega \text{ cm}^2$)	C_{LF} (F cm^2)
Compound 5	25	1244	5.84×10^{-10}	368	2.24×10^{-3}
	50	1048	1.17×10^{-9}	1186	7.63×10^{-5}
	100	1395	7.44×10^{-10}	1687	9.61×10^{-5}
Compound 6	25	1392	9.14×10^{-10}	558	5.39×10^{-5}
	50	1109	1.45×10^{-9}	838	6.81×10^{-5}
	100	1543	3.42×10^{-9}	2225	1.73×10^{-5}
Compound 7	25	1125	7.28×10^{-10}	176	7.00×10^{-5}
	50	972	3.09×10^{-9}	620	8.69×10^{-5}
	100	1571	3.90×10^{-9}	7252	2.73×10^{-5}
Blank (no inhibitor)		377	1.28×10^{-7}	436	1.75×10^{-3}

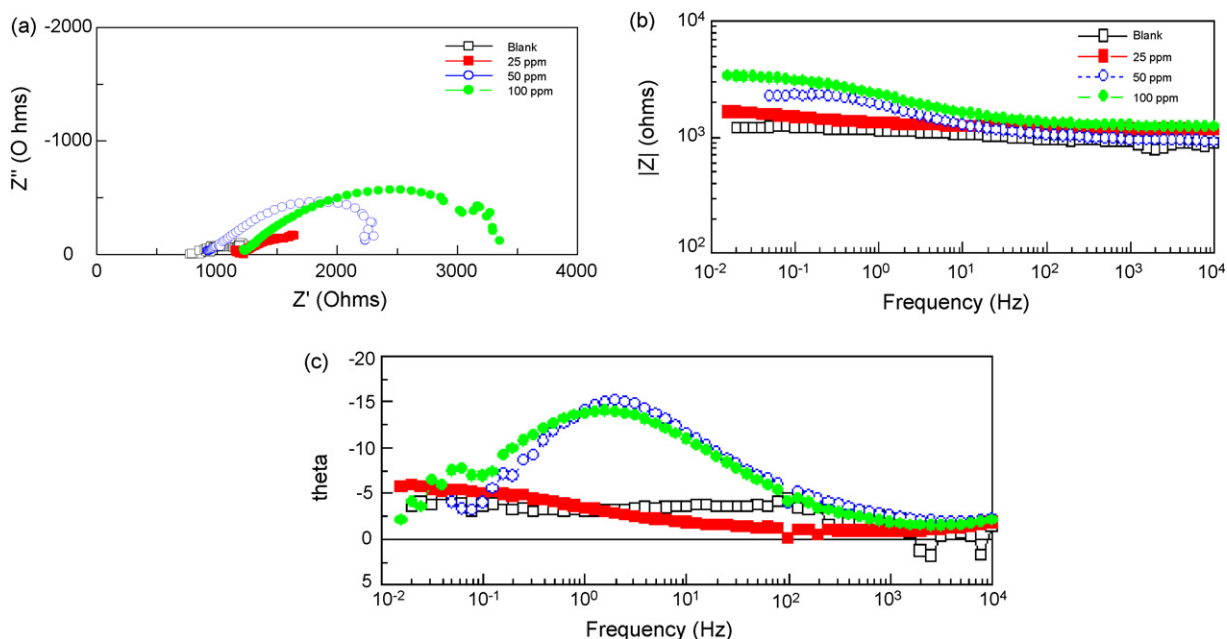


Fig. 4. Impedance diagram: (a) Nyquist plots and (b) Bode modulus. (c) Bode phase angle plots diagrams for API 5L-X steel in white petrol–water mixtures containing different concentrations AAQ derivative of compound 5.

clearly defined, but the corresponding to the low frequency (LF) range was well defined. The HF time constant was attributed to the contribution of the intact part of the adsorbed film to the total system impedance, whereas the LF data points were associated with the Faradaic process occurring on the bare metal through defects and pores [39–41] in the adsorbed inhibitor layer. Nyquist plots of API 5L-X60 in white petrol–water mixtures were analysed by using the equivalent circuits represented in Fig. 7. In the case of 100 ppm of compounds **6** and **7**, an inductive loop was observed in the lower frequency area. This is due to the movement of ions between inhibitor film (compounds **6** and **7**) and the

metal surface. The corresponding equivalent circuit is represented in Fig. 7b.

The respective Bode modulus plots are shown in Figs. 4b, 5b and 6b. The electrode impedance greatly increased from 25 ppm to 100 ppm when compared to control (blank) experiment. The Bode phase angle versus log frequency plots, Figs. 4–6, shows the phase shift in the high frequency side for 100 ppm of AAQ derivatives (compounds **5**–**7**), which is an indication of the inhibitive nature of the synthesized compounds [42,43]. This is in agreement with the results of polarization data. The capacitance values were lower in all inhibitor addition systems when compared

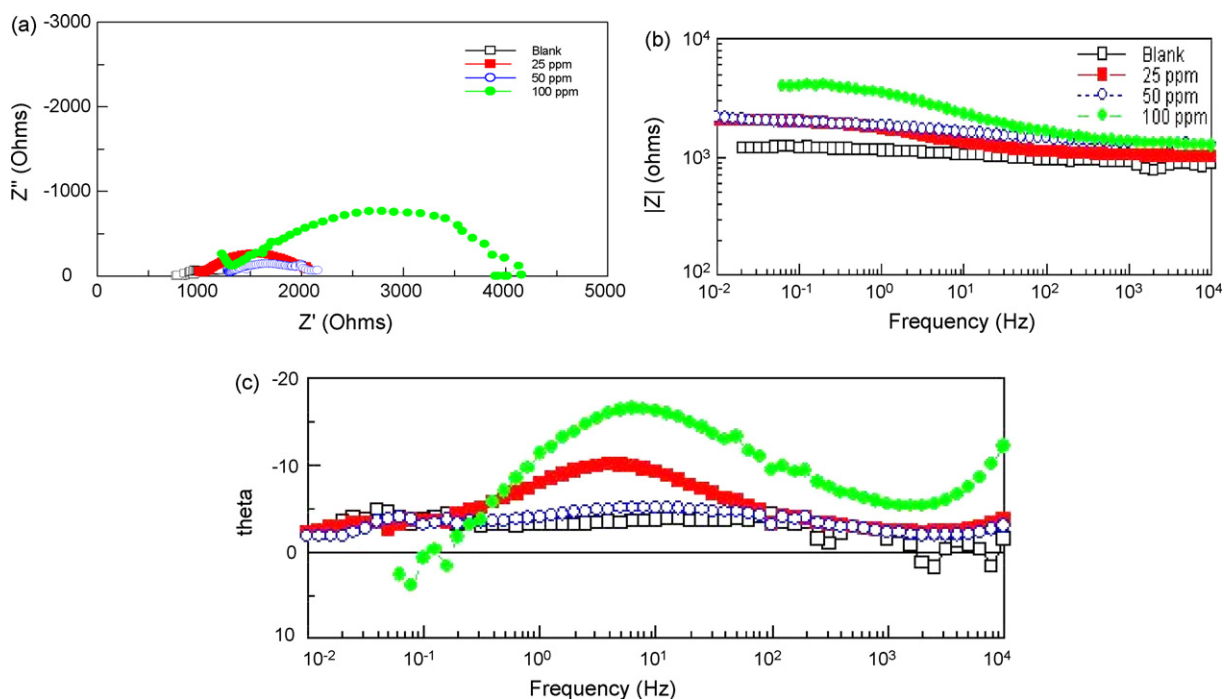


Fig. 5. Impedance diagram: (a) Nyquist plots and (b) Bode modulus. (c) Bode phase angle plots diagrams for API 5L-X steel in white petrol–water mixtures containing different concentrations AAQ derivative of compound 6.

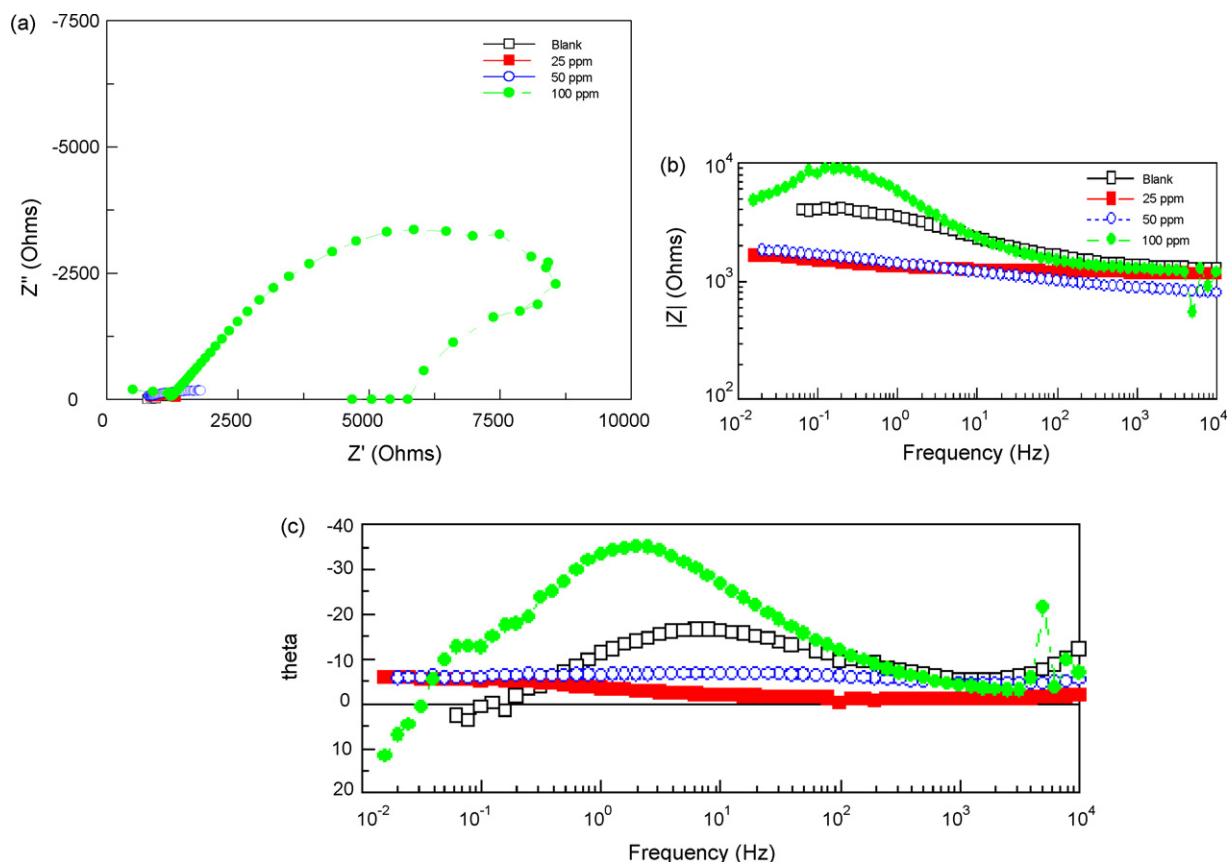


Fig. 6. Impedance diagram: (a) Nyquist plots and (b) Bode modulus. (c) Bode phase angle plots diagrams for API 5L-X steel in white petrol–water mixtures containing different concentrations AAQ derivative of compound 7.

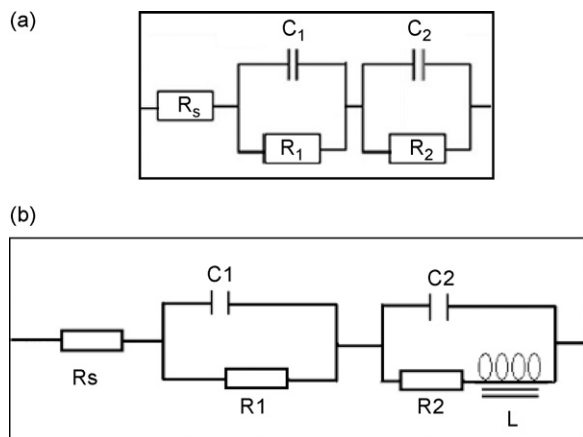
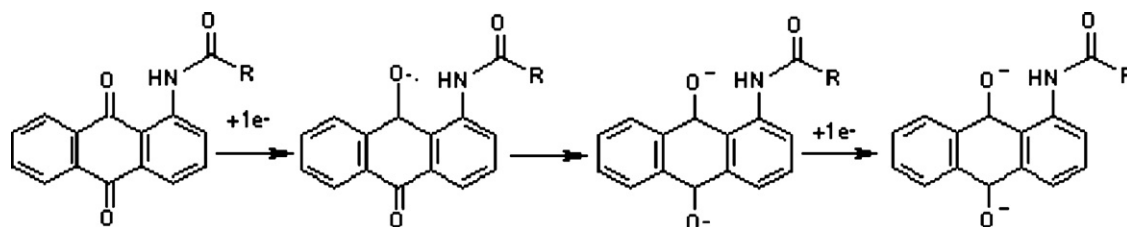


Fig. 7. Corresponding equivalent circuit for API 5L-X60 in white petrol–water system: (a) in test system of 25–100 ppm containing compound 5 and 25 ppm and 50 ppm of compounds 6 and 7; (b) in test system of 100 ppm containing compounds 6 and 7.



Scheme 3. Redox activity nature of 1-aminoanthraquinone derivatives (formation of semiquinone and hydroquinone).

to control. It also confirms that the adsorbed film reduced the dielectric constant present on the metal surfaces. The decrease of capacitance values in the presence of inhibitors such as propyl amine (PA) and isopropyl amine (i-pA) for steel in petroleum–water mixture medium was reported by many investigators [44–46]. The reduction in capacitance could be accounted for the decrease in local dielectric constant and/or an increase in thickness of the electrical double layer. It reveals that the inhibitors adsorb at the metal–solution interface [47,48].

3.5. AFM measurement

Atomic force microscope is a powerful technique for characterizing the surface morphology [49–52]. The adsorption process due to the action of 1-aminoanthraquinone derivatives (compound 7) was monitored with an AFM after 8 h immersion time and presented in Figs. 8 and 9. The surface morphology of the sample before exposure to 1-aminoanthraquinone derivatives is presented in Fig. 8. Fig. 9 shows a thin and covering surface film composed of many particles. Fig. 9a shows the spherical or bread-like particles appear on the surface, which does not exist in Fig. 8a. Investigation by

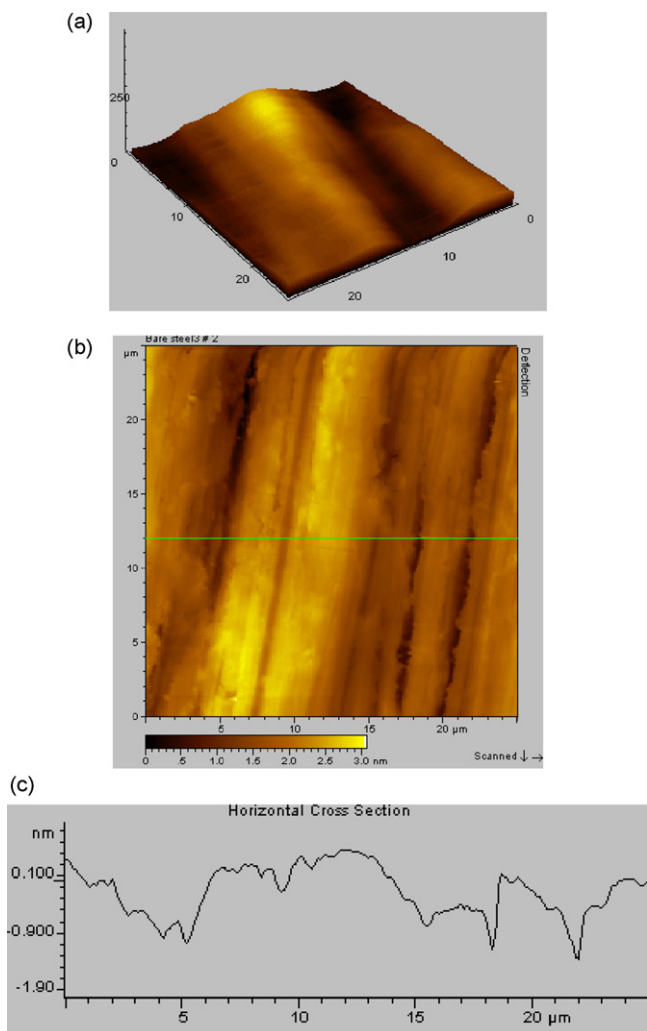


Fig. 8. Cross-sectional profiles of the API 5L-X60 surface in white petrol–water mixture: (a) in the absence of 1-aminoanthraquinone (AAQ) derivatives (3D view), (b) surface topography of API 5L-X60 in absence of AAQ derivative (2D view) and (c) height profile of the API 5L-X60 surface, which is made along the line marked in corresponding (b).

Table 4

Bacterial count in presence of AAQ derivatives (compounds 5–7) in white petrol–water interface.

Sl. no.	Compound	Total viable count (CFU ml ⁻¹)	
		<i>Serratia marcescens</i> ACE2	<i>Bacillus cereus</i> ACE4
1	Control (without AAQ)	7.63×10^9	6.89×10^9
2	Compound 5	1.77×10^3	4.73×10^4
3	Compound 6	5.46×10^2	5.63×10^3
4	Compound 7	1.58×10^2	2.57×10^2

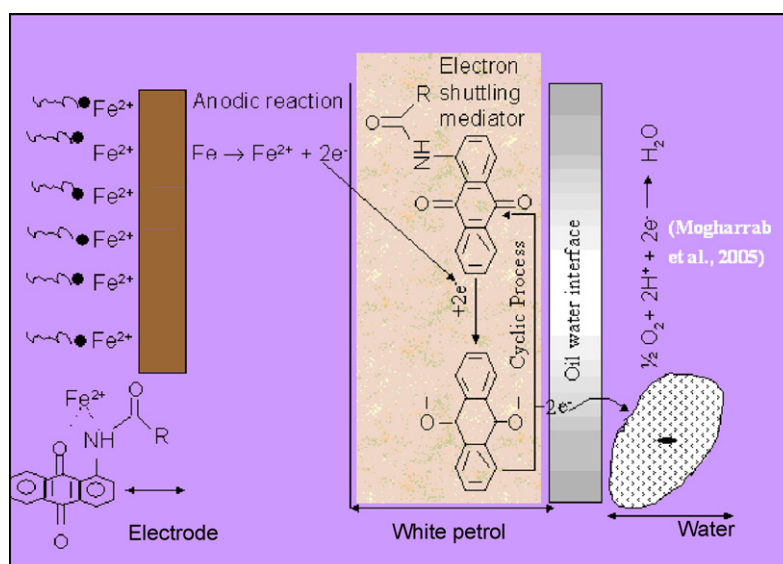
Leng and Stratmann [53] suggested that adsorption of corrosion inhibitors may form a few protective monolayers. These particles may be mainly composed of the adsorbed 1-aminoanthraquinone derivative molecules.

3.6. Antimicrobial efficacy

After 24 h incubation period, the total viable bacterial counts (TVC) of the 1-aminoanthraquinone derivatives against *S. marcescens* ACE2 and *B. cereus* ACE4 are listed in Table 4. All of the AAQ showed biocidal properties against the bacteria. Compounds 5–7 reduced the counts from 10^8 CFU ml⁻¹ to 10^9 CFU ml⁻¹ to 10^2 CFU ml⁻¹ of *S. marcescens* and *B. cereus* at 100 ppm. The observation shows that if the alkyl chain of 1-aminoanthraquinone derivatives contained less than eight carbons, they showed weak antibacterial activities these findings agree well with other reports [54–56]. It is also interesting to note that the 1-aminoanthraquinone derivatives generally showed better antimicrobial efficacy against *S. marcescens* than *B. cereus*. Gram-positive bacteria (*B. cereus*) show greater resistance to mechanical rupture than Gram-negative cells (*S. marcescens*). Because, Gram-positive bacteria, the main component of the cell walls is a rigid network composed of three macromolecular concentric shells, while Gram-negative bacteria have a network that is only one molecule thick, together with up to 25% (mass) of lipoprotein and lipopolysaccharide [57].

3.7. Analysis of X-ray diffraction patterns

The X-ray diffraction patterns of the film formed on surface of the mild steel specimens immersed in various test solutions are given in Fig. 10. The peak due to iron appeared at $2\theta = 43.80^\circ$, peaks



Scheme 4. Enlarge view of inhibitor adsorption on API 5L-X60 in white petrol–water mixtures.

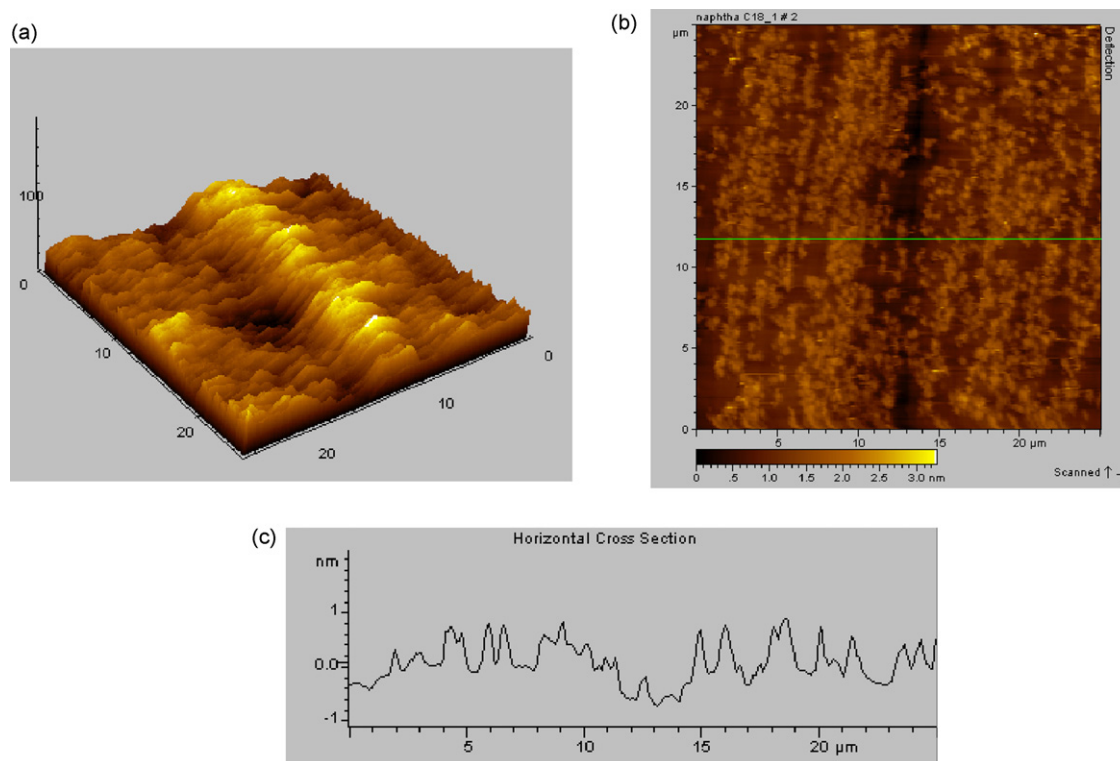


Fig. 9. AFM pictures of the morphology of the electrode (API 5L-X60) obtained after 8 h of immersion in white petrol–water mixture of AAQ derivative (compound 7) at 50 ppm: (a) in the presence of 1-aminoanthraquinone (AAQ) derivative (3D view), (b) surface topography of API 5L-X60 in presence of AAQ derivative (2D view) and (c) height profile of the API 5L-X60 surface, which is made along the line marked in corresponding (b).

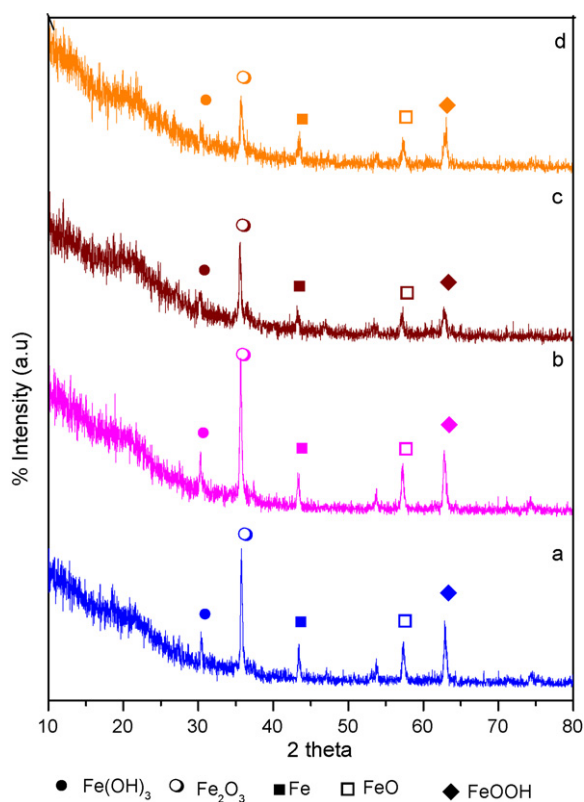


Fig. 10. XRD pattern obtained on the surface film formed on API 5L-X60 steel at the end of 10 days in different environment. Curves: (a) blank, (b) 50 ppm of compound 5, (c) 50 ppm of compound 6 and (d) 50 ppm of compound 7.

at $2\theta = 30.4^\circ$, 36° and 62.4° were assigned to iron oxides. In the case of steel pipes immersed in white petrol–water mixtures, those were mainly $\text{Fe}(\text{OH})_3$, Fe_2O_3 and FeOOH . The XRD pattern of the surface of the alloy immersed in the solution containing 50 ppm AAQ derivatives (compound 5–7) are given in Fig. 10b–d. It is observed that the peaks due to iron oxides such as Fe_2O_3 and FeOOH showed less intensity than the corresponding to the control material (Fig. 10a).

3.8. Mechanism of inhibition

Generally all petroleum product pipelines have water contamination in the range between 2% and 11%. A tentative mechanism is proposed for the observed corrosion inhibition phenomena. The white petrol–water in pipeline is considered as three layers. First layer is considered as pipeline (electrode), the synthesized derivatives dissolved in white petrol medium were considered as a second layer. The third layer was white petrol–water interface.

It is well known that iron dissolves as Fe^{2+} from first layer at anodic area (Eq. (2)). This reaction is rapid in most media [58]:



Due to the redox active nature of synthesized compounds 5–7, it can take the anodically produced two electrons and form semiquinone and hydroquinone [28] at the second layer (Scheme 3). Further the hydroquinone loses two electrons and returns to the original state of quinone in a cyclic process. The two electrons are consumed by bacteria for respiratory process at the third layer (Scheme 4). In the present study, the movement of ions on the metal surface was observed in the impedance spectroscopy. The interaction of quinone model compounds or humus substances with the bacterial life cycle has already been reported by Cervantes et al. [59–61]. The anodically produced Fe^{2+} ions could coordinate with compounds 5–7 using the hetero (nitrogen and oxygen) atoms present. Subsequently due to the lack of electrons from the anodic

spot, the cathodic reaction is suppressed. The inhibition effect of these compounds is attributed to the adsorption of the inhibitor molecules on the metal surface. It can be concluded that the fatty acid derivatives of 1-aminoanthraquinone in white petrol–water system inhibits corrosion due to the adsorption of these compounds on the steel surface through their lone pair of electrons and π electrons of the aromatic ring. All the studied 1-aminoanthraquinone derivatives 5–7 shows the inhibition efficiency ranging from 36% to 84% in the concentration range of 25 ppm, 50 ppm and 100 ppm. It can be noticed that when the inhibitor concentration increased, the resistance of inhibitor layer increased. Thus, at 25 ppm concentration, the octanoic acid substituted 1-aminoanthraquinone showed lower efficiency in comparison with other inhibitors due to less surface coverage. The increase in carbon chain increased the corrosion inhibition efficiency. The order of inhibitor efficiency is compound 5 (C_8) < compound 6 (C_{10}) < compound 7 (C_{18}).

4. Conclusion

We have successfully demonstrated that fatty acid derivatives of 1-aminoanthraquinone can be used as corrosion inhibitor for steel API 5L-X60 in white petrol–water mixtures. Inhibition efficiency increases with increase in concentration of 1-aminoanthraquinone derivatives. Among the derivatives 5–7, oleic acid substituted 1-aminoanthraquinone (compound 7) was found to be a good inhibitor for carbon steel (API 5L-X60) corrosion in white petrol–water mixtures. The results obtained from electrochemical studies were in good agreement with those obtained from weight loss measurements. EIS measurements indicated the single charge transfer process controlling the corrosion of iron. They bring down the corrosion rate by adsorption mechanism. AFM studies also confirmed the film formation of the synthesized compounds (compounds 5–7) on the metal surface. All the 1-aminoanthraquinone derivatives, 5–7 exhibited antimicrobial efficacy against *S. marcescens* ACE2 and *B. cereus* ACE4.

Acknowledgements

The authors wish to express their thanks to The Director, CECRI, Karaikudi 630006, for his kind permission. One of the authors N.M. thanks CSIR–HRDG for the award of Senior Research Fellowship. The authors are thankful to Dr. S. Sathyanarayanan, Dr. J. Mathiyarasu and Mr. S.P. Manoharan for help rendered in electrochemistry and AFM experiments respectively.

References

- [1] W. Durnie, B. Kinsella, R. De Marco, A. Jefferson, J. Electrochem. Soc. 146 (1999) 1751.
- [2] F. Bentiss, M. Lagrenée, M. Traisnel, Corrosion 56 (2000) 733.
- [3] V.S. Sastri, Corrosion Inhibitors Principles and Applications, John Wiley & Sons, New York, 1998.
- [4] E.C. French, Mater. Perform. 37 (1978) 20.
- [5] I.L. Rosenfeld, Corrosion Inhibitors, McGraw-Hill, New York, 1981.
- [6] H.H. Uhlig, R.W. Rivie, Corrosion and Corrosion Control, John Wiley & Sons, New York, 1985.
- [7] P.J. Clewlow, J.A. Haselgrave, N. Carruthers, EP Patent 0,526,251 A1 (1992).
- [8] B. Sanyal, Progr. Org. Coat. 9 (1981) 165.
- [9] R.W. Revie (Ed.), Uhlig's Corrosion Handbook, 2nd edition, John Wiley & Sons, New York, 2000.
- [10] W. Frenier, F.B. Growcock, V.R. Lopp, Corrosion 44 (1988) 590.
- [11] F.B. Growcock, W.W. Frenier, Proc. Electrochem. Soc. 86–87 (1986) 104.
- [12] A. Cizek, Mater. Perform. 33 (1991) 56.
- [13] R.F. Monroe, C.H. Kucera, B.D. Oates, US Patent 3,007,454 (1963).
- [14] B.J. Little, P.A. Wagner, F. Mansfeld, Microbiologically Influenced Corrosion, NACE International, Houston, TX, 1997.
- [15] D.H. Pope, E.A. Morris III, Mater. Perform. (1995) 23.
- [16] N. Muthukumar, S. Mohanan, S. Maruthamuthu, P. Subramanian, N. Palaniswamy, M. Raghavan, Electrochem. Commun. 5 (2003) 421.
- [17] A. Navarro, Molec. Aspect Med. 25 (2004) 37.
- [18] R.M. Christie, Colour Chemistry, RSC, Cambridge, UK, 2001.
- [19] B. Kampmann, Y. Lian, K.L. Klinkel, P.A. Vecchi, H.L. Quiring, C.C. Soh, A.G. Sykes, J. Org. Chem. 67 (2002) 3878.
- [20] P. Terech, R.G. Weiss, Chem. Rev. 97 (1997) 3133.
- [21] S. Norvez, F.-G. Tournilhac, P. Bassoul, P. Herson, Chem. Mater. 13 (2001) 2552.
- [22] V. Prasad, K. Krishnan, V.S.K. Balagurusamy, Liq. Cryst. 27 (2000) 1075.
- [23] K.S. Raja, V.A. Raghunathan, S. Ramakrishnan, Macromolecules 31 (1998) 3807.
- [24] K. Krishnan, V.S.K. Balagurusamy, Liq. Cryst. 27 (2000) 991.
- [25] S. Kumar, J.J. Naidu, Liq. Cryst. 29 (2002) 1369.
- [26] S. Kumar, J.J. Naidu, S.K. Varshney, Liq. Cryst. 30 (2003) 319.
- [27] M.A. Tius, J. Gomezgaleno, X.Q. Gu, J.H. Zaidi, J. Am. Chem. Soc. 113 (1991) 5775.
- [28] N. Mogharrab, H. Ghourchian, Electrochem. Commun. 7 (2005) 466–471.
- [29] T.P. Hoar, R.P. Khera, Proceedings of the European Symposium on Corrosion Inhibitors, University of Ferrara, N.S. Sez. V, Suppl. 3, 1961, p. 73.
- [30] Annual Book of ASTM standards 2001, in: Standard Practice for Preparation, Cleaning and Evaluating Corrosion Test Specimens (G 1–90), Section 03.02, pp. 15–22.
- [31] S. Papavinasam, R.W. Revie, M. Attard, A. Demoz, H. Sun, J.C. Donini, K.H. Michaelian, Mater. Perform. 39 (8) (2000) 58.
- [32] D.W. Marquardt, J. Soc. Indust. Appl. Math. 11 (1963) 431.
- [33] E. Rodriguez de Schiapparelli, B.R. de Meybaum, Mater. Perform. 19 (1980) 47.
- [34] J.J. Kaminski, M.M. Hyycke, S.H. Selk, N. Bodor, T. Higuchi, J. Pharm. Sci. 65 (12) (1976) 1737.
- [35] R.D. Desai, R.N. Desai, J. Indian Chem. Soc. 33 (1956) 559–560.
- [36] H.S. Huang, H.F. Chiu, A.L. Lee, C.L. Guo, C.L. Yuan, National Defense Medical Center, School of Pharmacy, Taipei, Taiwan, Bioorg. Med. Chem. 12 (2004) 6163–6170.
- [37] M. Ma, Y. Sun, G. Sun, Dyes Pigments 58 (2003) 27–35.
- [38] T. Philipova, C. Ivanova, Y. Kamdzhilov, M.T. Molina, Dyes Pigments 53 (2002) 219.
- [39] I.D. Raistrick, Electrochim. Acta 35 (1990) 1579.
- [40] H.A. Sorkhabi, S.A. Nabavi-Amri, Electrochim. Acta 47 (2002) 2239.
- [41] H.A. Sorkhabi, T.A. Aliyev, S. Nasiri, R. Zareipoor, Electrochim. Acta 52 (2007) 5238.
- [42] A. Popova, E. Sokolova, S. Raicheva, M. Christov, Corros. Sci. 45 (2003) 33.
- [43] A.P. Yadav, A. Nishikata, T. Tsuru, Corros. Sci. 46 (2004) 169.
- [44] Y. Chen, W.P. Jepsen, Electrochim. Acta 44 (1999) 4453.
- [45] A. Hassanzadeh, A.Z. Isafahani, K. Movassaghi, H.A. Sorkhabi, Acta Chim. Slov. 51 (2004) 305.
- [46] T. Hong, Y. Chen, Y.H. Sun, W.P. Jepsen, Mater. Corros. 52 (2001) 590.
- [47] E. McCafferty, N. Hackerman, J. Electrochem. Soc. 119 (1972) 146.
- [48] K.F. Khaled, N. Hackerman, Electrochim. Acta 48 (2003) 2715.
- [49] A.A. Gewirth, B.K. Niece, Chem. Rev. 97 (1997) 1129.
- [50] I.C. Oppenherm, D. Trevor, C.E.D. Chidsey, P.L. Trevor, K. Sieradzki, Science 254 (1991) 688.
- [51] J. Li, D. Lampner, Colloids Surf. A 154 (1999) 227.
- [52] H.H. Teng, P.M. Dove, C.A. Orme, J.J. De Yoreo, Science 282 (1998) 724.
- [53] A. Leng, M. Stratmann, Corros. Sci. 34 (1993) 1657.
- [54] M. Pavlikova-Moricka, I. Lacko, F. Devinsky, L. Masarova, D.M. Folia, Microbiology 39 (3) (1994) 176.
- [55] F. Devinsky, A. Kopecka-leitmanova, F. Sersen, P. Balgavy, J. Pharm. Pharmacol. 42 (1990) 790.
- [56] F. Gregan, J. Oremusova, M. Remko, J. Gregan, D. Mlynarcik, II Farmaco 53 (1998) 41.
- [57] W.B. Hugo, J. Appl. Bact. 30 (1) (1967) 17.
- [58] J.C. Scully, The Fundamentals of Corrosion, 3rd edition, Pergamon Press, Oxford, UK, 1990.
- [59] F.J. Cervantes, Quinones as Electron Acceptors and Redox Mediators for the Anaerobic Biotransformation of Priority Pollutants, Wageningen University, The Netherlands, 2002, p. 162. ISBN 90-5808-567-8.
- [60] F.J. Cervantes, S. van der Velde, G. Lettinga, J.A. Field, FEMS Microbiol. Ecol. 34 (2000) 161.
- [61] F.J. Cervantes, W. Dijkema, T. Duong-Dac, A. Ivanova, G. Lettinga, J.A. Field, Appl. Environ. Microbiol. 67 (2001) 4471.